Letters in Applied NanoBioScience
Open-Access Journal (ISSN: 2284-6808)

Article
Volume 15, Issue 2, 2026, 57
https://doi.org/10.33263/LIANBS152.057

Lemongrass Oil-Based Microemulgel of Luliconazole: Formulation and Antifungal Assessment

Ujjwala Kandekar [1,*], Laxmi Suryawanshi [1], Sudha Mehetre [1], Ashlesha Pandit [1]

[1] Department of Pharmaceutics, JSPM's Rajarshi Shahu College of Pharmacy and Research, Tathawade, Pune-411033, Maharashtra, India
* Correspondence: uy_kandekar@jspmrscopr.edu.in;

Received: 23.07.2025; Accepted: 24.02.2026; Published: 30.06.2026

Abstract: This research work is focused on the development of luliconazole-loaded microemulgel using lemongrass oil to enhance its topical delivery. Different microemulsion formulations were prepared based on pseudoternary phase diagrams by varying the amounts of lemongrass oil, Labrasol, and Labrafil M 2125 CS, and evaluated. An optimized formulation was selected based on systematic comparison of evaluation parameters, loaded into 1% Carbopol 940 gel, and examined. pH, viscosity, drug content, and *in-vitro* diffusion for microemulsions ranged from 5.1±0.15 to 5.6±0.11, 41±1.5 to 48±1.5 cP, 97±0.21 to 98±0.67%, and 58±1.82 to 86±2.18%, respectively. Among four formulations, the F1 formulation was selected as the optimized formulation as it exhibits pH, viscosity, and drug content of 5.4±0.10, 41±1.5, and 98±0.44%, respectively. Results showed that optimized microemulsion exhibited pH, viscosity, drug content, and drug diffusion of 5.4±0.10, 41±1.5cP, 98±0.44%, and 86±2.18%, respectively. Particle size and zeta potential of optimized microemulsion were 187.9nm and -34.4mV, respectively. pH, viscosity, drug content, in-vitro diffusion, and *ex-vivo* diffusion of microemulgel were 6.0±0.11, 10032±1.5cP, 98±0.44%, 71±0.95%, and 68±2.06%, respectively. Zone of inhibition for the prepared microemulgel and the marketed gel was 29 and 26mm, respectively. These results demonstrated that the combination of luliconazole with lemongrass oil in an emulsion formulation enhanced antifungal activity.

Keywords: Luliconazole; lemongrass oil; microemulsion; microemulgel.

1. Introduction

"Mycoses" are fungal infections of the skin [1]. Every year, fungal infections caused by the *species Candida* detrimentally affect around 1.5 million individuals [2,3]. The reason for inflammatory lesions known as superficial candidiasis is the ability of *Candida* to adhere to epithelial cells, multiply, and filamentate [4]. Although these infections can develop on nearly any part of the body, they are more prevalent in intertriginous areas, where two skin surfaces may come into contact or rub against one another [5,6]. For the treatment of fungal infections, five antifungal classes are currently available: azoles, echinocandins, allylamines, polyenes, and pyrimidine analogs. Among these, azole antifungals are usually used for treating candidiasis. Biosynthesis of ergosterol is restricted by these agents, as azoles block the enzyme 14α-sterol demethylase, preventing the conversion of lanosterol into ergosterol and impairing the synthesis of fungal membranes [3]. Broad-spectrum antifungal azole derivative

luliconazole acts by a similar mechanism, but it suffers from restricted solubility [7]. Components of lemongrass essential oil, such as geraniol, citral, limonene, myrcene, and linalool, exhibit strong antifungal properties. Geraniol enhances potassium ion efflux from fungal cells, whereas citral disrupts microtubule structures and reduces fungal viability. Monoterpene alcohol linalool has variety of fungicidal effects. Moreover, other aldehydes present in lemongrass essential oil may exert antifungal effects by forming cross-links within the fungal cell membrane [8]. In combination with antifungal agents, lemongrass oil is responsible for enhancing the antifungal activity and reducing overall resistance. Promoting the leakage of the cell membrane of the fungal cell wall, it also enhances the permeability of antifungals in fungal cells. Labrasol (Caprylocaproyl Polyoxyl-8 glycerides) and Labrafil M 2125 CS (Linoleoyl Polyoxyl-6 glycerides) are non-ionic surfactants and cosurfactants, respectively. Labrasol weakens interfacial forces between oil and aqueous layers, allowing fine dispersion of oil droplets containing lipophilic drug. Labrafil M 2125 CS inserts between surfactant molecules at interface, increasing flexibility of interfacial film and improving droplet stability. Lipophilic drugs are solubilized in oily core of microemulsion droplets, protected by a surfactant-cosurfactant layer, and form a clear and stable microemulsion (ME). Carbopol 940 creates viscous, smooth, and stable gels. Its matrix-forming ability can help sustain or control release of drug from the gel, improving therapeutic outcomes.

Microemulsions are isotropic, clear liquid systems that remain thermodynamically stable and are formed from oil, water, and surfactants, often with a cosurfactant added. Microemulgel is a term used to describe formulations that combine the benefits of both microemulsions and emulsions. Incorporation of microemulsion into the gel helps stabilize it, enhances its aesthetic appeal, and allows it to be easily washed off when necessary [9].

The objective of this study was to formulate and assess a microemulgel for the topical delivery of luliconazole, incorporating lemongrass oil as the oil phase. The microemulsion was converted to a microemulgel to increase the drug's contact time with the skin, improving absorption and prolonging the antifungal effect.

2. Materials and Methods

2.1. Materials.

Luliconazole was purchased from Swapnroop Drugs and Pharmaceuticals Ltd., India. Lemongrass oil was obtained from Nisarg Biotech Pvt. Ltd., Maharashtra, India. Labrasol and Labrafil M 2125 CS were generously gifted by Gattefosse Ltd., India. Carbopol 940 and Triethanolamine were procured from Thermosil Fine Chem Industries, Maharashtra, India. Potassium dihydrogen ortho phosphate, methanol, and sodium hydroxide were purchased from Thermosil Fine Chem Industries, India.

2.2. Methods.

2.2.1. Drug-excipient compatibility study by ATR-FTIR.

The compatibility between the drug and excipients was studied by ATR-FTIR spectroscopy. Briefly, Luliconazole, lemongrass oil, Labrasol, and Labrafil M 2125 CS were thoroughly mixed in a 1:1 ratio. This mixture was subjected to 40°C at 75% RH for one month and scanned by ATR-FTIR in the wavelength range of 4000 to 400cm^{-1}.

2.2.2. Solubility of luliconazole in oil, surfactant, and cosurfactant.

The shake flask method is used to assess the solubility of luliconazole in oil (lemongrass oil), surfactant (Labrasol), and cosurfactant (Labrafil M 2125 CS). Solubility was assessed by dissolving an excess amount of the drug in lemongrass oil, Labrasol, and Labrafil M 2125 CS, separately. Mixtures were then continuously stirred in an orbital shaker (Bio Techniques India, Maharashtra, India) at 75rpm for 48h, followed by centrifugation in a high-speed centrifuge (C-24 plus, Remi Electrotechnik Ltd, India) for 15min at 5000rpm [10]. Supernatant was collected, diluted with methanol, filtered using Whatman filter paper (45µ), and subjected to analysis using a UV-Visible spectrophotometer (UV 1800, Shimadzu Corporation, Kyoto, Japan) at 296nm [11]. Triplicate (n=3) determinations were carried out for each measurement.

2.2.3. Construction of pseudoternary phase diagram.

Development of a pseudoternary phase diagram was carried out via the water titration method by Ternary plot software (TernaryPlot.com). Labrasol and Labrafil M 2125 CS were blended at different weight proportions, 1:1, 2:1, 3:1, 4:1, 5:1, 6:1, 7:1, and used as S_{mix}. For each phase diagram, the ratio of oil to S_{mix} was 1:9, 2:8, 3:7, 4:6, 5:5, 6:4, 7:3, 8:2, 9:1 (% w/w), respectively [12]. Then water was gradually added to each oil–S_{mix} blend with continuous vigorous stirring till it forms a clear homogeneous phase to determine the microemulsion region. Component concentrations at this stage were documented to build a pseudoternary phase diagram [13].

2.2.4. Formulation of microemulsion.

The Smix ratio of 7:1 showed a higher microemulsion region. Hence, selected further for the formulation of a microemulsion [14]. Once the microemulsion region was determined from the phase diagram, formulations were developed accordingly at different oil-to-Smix ratios. Luliconazole was added to oil, then Smix was added to this mixture. Mixtures were stirred at room temperature using a magnetic stirrer (Bio Techniques, India). Then water was added drop by drop to these mixtures until it became clear and transparent [13]. The composition of microemulsion formulations is shown in Table 1.

Table 1. Composition of microemulsion.

Formulation	Oil (%)	S_{mix} (%)	Water (%)	Drug (% w/w)
F1	5.56	50.00	44.44	1
F2	13.11	52.46	34.33	1
F3	22.64	52.83	24.53	1
F4	28.07	42.11	29.82	1

2.3. Characterization of microemulsion.

2.3.1. Determination of pH, viscosity, and drug content.

pH values were recorded using a digital pH meter (Labman Scientific Instruments Pvt. Ltd., India) [15]. Viscosity measurements of microemulsion were performed with LVDVE Brookfield digital viscometer (Brookfield Engineering Corporation, Massachusetts, USA) using spindle number 63 at 60rpm in triplicate (n=3) [16]. To determine the drug content, microemulsion (20mL, containing 200mg luliconazole) was dissolved in methanol, and the final volume was brought up to 100mL, followed by stirring for 10min. [17]. The solution was filtered through Whatman filter paper (45µm), and the absorbance of the filtrate was

spectrophotometrically analyzed at 296nm in three replicates [11]. Drug content was calculated as shown in equation (1).

$$Drug\ content\ (\%) = \frac{Actual\ amount\ of\ luliconazole}{Theoretical\ amount\ of\ luliconazole} \times 100 \quad (1)$$

2.3.2. In-vitro drug diffusion study.

Franz diffusion cell apparatus was utilized to perform an *in vitro* drug diffusion study in triplicate (n=3, DBK diffusion cell apparatus, DBK Instruments, India) using a cellophane membrane (HiMedia Laboratories, 150LA401, molecular weight cut-off of 12-14 kDa, India). Phosphate buffer (pH 7.4) and methanol mixture in a 9:1 ratio [18] served as diffusion medium (20mL) maintained at 37±5°C. A cellophane membrane was fixed between the donor and receiver compartments. Freshly prepared luliconazole-loaded microemulsion 1mL (10mg/mL) was placed on a cellophane membrane, and the stirring speed was set at 100 rpm to agitate the receptor fluid. Then, 1mL aliquot was periodically removed from receptor chambers at time intervals of 0.5, 1, 1.5, 2, 2.5, 3, 3.5, 4, 4.5, ……..7, 7.5, 8h and replaced with 1mL of phosphate buffer and methanol mixture (9:1) to adjust sink conditions. Samples were analyzed at 296nm spectrophotometrically [11].

2.4. Selection and evaluation of optimized formulation.

Among the F1, F2, F3, and F4 formulations, the formulation with the highest percent of drug diffusion, pH, drug content, and microemulsion viscosity was selected as the optimized formulation.

2.4.1. Analysis of particle size, Polydispersity index (PDI), and zeta potential.

Microemulsion (0.1 mL) was suitably diluted in 10 mL of Milli-Q deionized water (Direct-Q, Merck KGaA, Darmstadt, Germany). Measurements of particle size and PDI were performed with Malvern Zetasizer (ZEN1002, Malvern Zetasizer Lab. United Kingdom) at 25°C, with a scattering angle of 90° based on the dynamic light scattering technique [19].

2.4.2. Differential scanning calorimetry (DSC).

A differential scanning calorimeter (Mettler Toledo, SW STAR, Mettler-Toledo International Inc., USA) was employed for thermal analysis of luliconazole and luliconazole-loaded microemulsion. Accurately weighed luliconazole (4.2mg) and luliconazole-loaded microemulsion (3.8mg) samples were placed in cuvettes separately with aluminum lids and heated from 20°C to 200°C at a rate of 10°C/min in a nitrogen blanket [20].

2.4.3. Scanning electron microscopy (SEM).

Microemulsion's surface morphology was studied through scanning electron microscopy analysis (SEM Quanta-200-EDX system, ICON Labs, Mumbai). One drop of microemulsion was placed on carbon tape, which was then attached to the stub and allowed to air dry. Subsequently, the sample was analyzed via a scanning electron microscope operating at 20kV voltage [21].

2.5. Formulation of microemulgel.

Carbopol 940 was dispersed in distilled water to prepare 1% w/v gel, followed by overnight hydration. Smooth and viscous gel was obtained by blending the prepared microemulsion and 1% Carbopol gel in a 1:1 ratio [22]. Then, pH was adjusted using triethanolamine.

2.6. Characterization of microemulgel.

2.6.1. Determination of pH, viscosity, and drug content.

pH of formulation was assessed by mixing gel (1g) with purified water (10mL) and measuring its pH with a digital pH meter [17]. Viscosity measurements of microemulsion were carried out using a Brookfield viscometer with spindle number 64 at 60rpm [23]. Drug content of microemulgel was determined by transferring the microemulgel containing 10mg of luliconazole to a 10mL volumetric flask. It was dissolved in methanol, stirred for 30min, and filtered using Whatman filter paper (45µ). Absorbance of the resulting solution was recorded for the prepared solution at 296 nm spectrophotometrically [11].

2.6.2. Texture analysis of microemulgel.

CT3 Texture Analyzer was employed to assess the spreadability of microemulgel in triplicate (n=3, CT3 Brookfield Engineering Labs Inc., USA). The female probe was carefully filled with the microemulgel formulation, ensuring the absence of air bubbles. With a diameter of 35mm and a 45° angle, an analytical male probe was inserted into every sample at a controlled rate of 1mm/s until reaching a depth of 10mm, with a trigger force of 2g. From the force-time plot, the work of adhesion was calculated [24].

2.6.3. *In-vitro* diffusion study.

Similar to the previously described *in-vitro* diffusion study, drug diffusion studies were carried out for pure luliconazole, luliconazole-loaded microemulsion, and luliconazole-loaded microemulgel.

2.6.4. *Exvivo* diffusion study.

The Franz diffusion cell apparatus served as a system for *ex vivo drug-diffusion studies of the* optimized formulation of microemulsion, microemulsion-loaded gel, marketed gel, and luliconazole plain gel. Goat skin was employed as a diffusion membrane. Freshly excised goat abdominal skin was gently rinsed with a cold saline solution and shaved to remove hair. Non-dermatome tissue was carefully excised using a scalpel. Precautions were taken to avoid making transverse cuts while removing hair and excess skin. Goat skin was fixed between the donor and recipient compartments so that the donor compartment faces the stratum corneum directly [24]. Freshly prepared 10mg/mL luliconazole-loaded microemulsion, microemulsion-loaded gel, marketed gel, and plain luliconazole gel were put on the skin separately and stirred at a speed of 100rpm to agitate receptor fluid. The rest of the study was performed similarly to the in-vitro diffusion study described above.

2.6.5. Antifungal activity.

The agar well diffusion method was employed to assess the antifungal activity of pure luliconazole, lemongrass oil, luliconazole-loaded microemulsion, luliconazole-loaded microemulgel, and marketed gel against *Candida albicans*. In brief, 100 mL of distilled water was mixed with 7g of nutrient agar in a 250mL conical flask. It was boiled till complete dissolution. The resultant solution was sterilized for 30 min at 15psi pressure at 121°C by using an autoclave (Space Lab Instruments, India). After sterilization, the agar solution was cooled, subsequently poured into sterilized petri plates, and allowed to solidify. Then, *Candida albicans* suspension was spread onto these solidified petri plates. A sterile cork borer (6mm) was used to punch wells into solidified agar. Then, samples were added to these wells separately, and agar plates were maintained at 37°C for 24h to allow incubation, followed by measurement of inhibition zones [25].

3. Results and Discussion

The present study was aimed at enhancing the solubility of luliconazole by the microemulsion approach. Besides, lemon grass oil was used to enhance the antifungal activity of the formulation. Literature studies revealed the antifungal activity of numerous essential oils. Clove oil and tea tree oil-based topical microemulsion gel have been studied in combination with luliconazole for topical antifungal delivery [26]. Eucalyptus and clove oil were also investigated for antifungal activity in combination with ketoconazole [27]. Clove oil was also used in combination with fluconazole to enhance its antifungal activity against *Candida albicans* in the microemulsion formulation [28]. This literature highlights the synergistic activity of antifungal agents in combination with essential oils. Hence, the current research work was based on a combination of luliconazole with lemon grass oil.

3.1. Drug-excipient compatibility study by ATR-FTIR.

Luliconazole showed characteristic peaks at 3035.11, 3178.51, 1689.19, and 1126.55cm^{-1} corresponding to C-H stretching, N-H stretching, C=N stretching, and C=O stretching, respectively (Figure 1A).

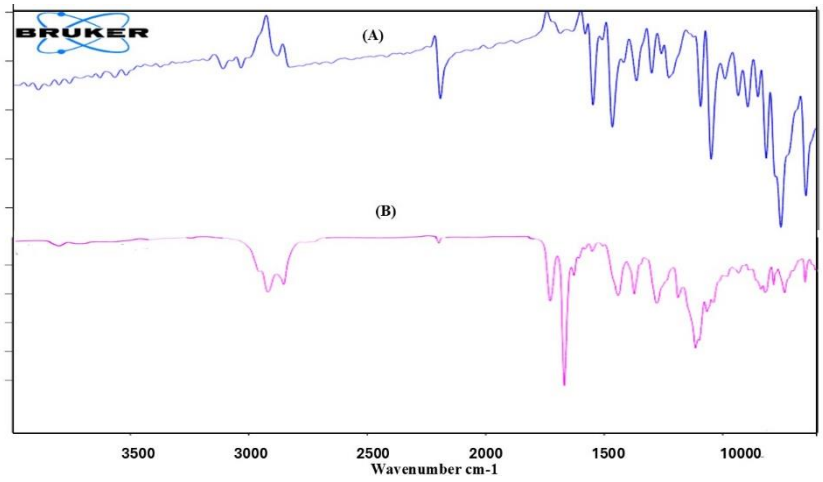

Figure 1. FTIR spectrum of **(A)** luliconazole; **(B)** physical mixture of luliconazole, lemon grass oil, Labrasol, and Labrafil M 2125 CS in a (1:1) ratio, indicating compatibility of these excipients with the drug.

ATR-FTIR spectrum of a physical mixture showed peaks at 2922.93, 2854.91, 1671.66, and 1119.29cm^{-1} corresponding to C-H stretching, N-H stretching, C=C stretching, C=N

stretching, and C=O stretching, respectively (Figure 1B). The peaks of luliconazole in the physical mixture were slightly shifted to lower wavelengths, indicating physical interaction between the drug and the excipients. These results confirmed the compatibility between the drug and the excipients.

3.2. Assessment of luliconazole's solubility.

Luliconazole was tested for solubility in lemongrass oil, Labrasol, and Labrafil M 2125 CS, with results noted as mentioned in Table 2. The concentration of the luliconazole in various solvents was determined by UV-Spectrophotometry, which was validated for accuracy, linearity, reproducibility, range, specificity, and robustness. The same instrument and method were used to carry out other methods that require UV analysis.

Table 2. Solubility of luliconazole in oil phase, surfactant, and co-surfactant.

Sr. no.	Component	Solvent	Solubility
1	Oil phase	Lemongrass oil	15.84±0.06mg/mL
2	Surfactant	Labrasol	9.72±0.39mg/mL
3	Cosurfactant	Labrafil M 2125 CS	12.44±0.30mg/mL

3.3. Construction of a pseudoternary phase diagram to prepare a microemulsion.

Each surfactant: cosurfactant ratio of 5:1 (Figure 1A), 6:1 (Figure 1B), and 7:1 (Figure 1C) was used to construct a pseudoternary phase diagram by plotting the concentration of oil, surfactant, and cosurfactant. Among these combinations, the 7:1 ratio showed a larger microemulsion zone, as it contained a higher surfactant-to-co-surfactant ratio. Surfactant molecules gather at the oil-water interface and reduce interfacial tension to ultra-low levels, facilitating the better solubilization of the oil and water phases into a stable microemulsion.

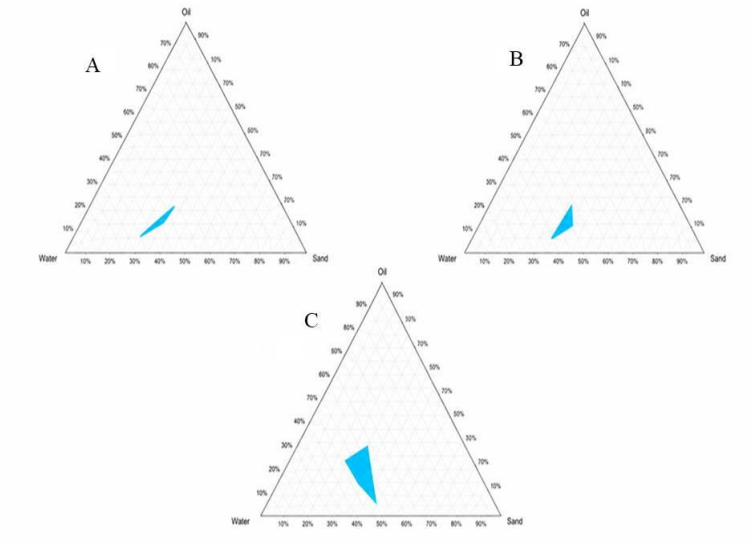

Figure 2. Pseudoternary phase diagrams of microemulsion with S_{mix} of **(A)** 5:1; **(**B**)** 6:1; **(C)** 7:1; Surfactant ratio 7:1 showed a higher microemulsion zone.

3.4. Characterization of microemulsion.

3.4.1. pH, viscosity, and drug content.

pH of all four microemulsion formulations ranged from 5.1±0.15 to 5.6±0.11, which is within the reported skin pH of 4.5 to 6 [29]. Viscosity plays a key role in stability and release

of the drug from the microemulsion. Viscosity ranged from 41±1.5 to 48±1.5cP (Table 3). Microemulsion formulation F4, which contained a higher proportion of oil, shows the highest viscosity (48±1.5). In contrast, formulation F1, with lower oil content and higher S_{mix} ratio, exhibited the lowest viscosity (41±1.5). Drug content of these four formulations was in the range of 97±0.21 to 98±0.67%, demonstrating maximum solubilization of luliconazole during formulation. This range complies with the British Pharmacopoeial requirement of 95-110%. Formulations F1 and F2 exhibited the highest drug content of 98±0.44 and 98±0.67%, respectively, indicating efficient incorporation of the antifungal agent [30]. In comparison, formulations F3 and F4 showed slightly lower drug content values of 97±0.13 and 97±0.21%. Slight variation observed among different formulations attributed to differences in oil and S_{mix} proportion. From F1 to F4, oil content increases, and Smix content decreases, resulting in a decrease in drug content. This is because S_{mix} plays a crucial role in stabilizing the microemulsion system and solubilizing the drug at the oil-water interface. High drug content also reflects thermodynamic stability and solubilization capacity of the microemulsion system.

Table 3. Evaluation parameters of microemulsion.

Formulation	pH	Viscosity (cP)	Drug content (%)
F1	5.4±0.10	41±1.5	98±0.44
F2	5.1±0.15	42±1.2	98±0.67
F3	5.3±0.17	44±1.6	97±0.13
F4	5.6±0.11	48±1.5	97±0.21

3.4.2. *In-vitro* diffusion study.

The Franz diffusion cell apparatus was employed for an *in-vitro* diffusion study, which was carried out for 8h. Among all formulations, F1 demonstrated the highest cumulative drug permeation through the membrane, which was 86±2.18% as compared to F2, F3, and F4 formulations (75±2.71, 63±2.19, and 58±1.82%, respectively) as shown in Figure 3. Formulation F1, F2, F3, and F4 followed Higuchi diffusion kinetics with R^2 values of 0.9664, 0.9687, 0.9792, and 0.9837, respectively. Water was selected as the external phase in o/w microemulsions and serves as the medium through which the drug diffuses. F1, with the highest water content, provides a more favorable environment for the drug to partition into the aqueous phase and diffuse across the membrane. S_{mix} facilitates the formation of microemulsions by reducing interfacial tension and stabilizing droplets. F1 and F2 have relatively higher S_{mix} content, promoting the formation of smaller and more stable droplets with a larger surface area for diffusion.

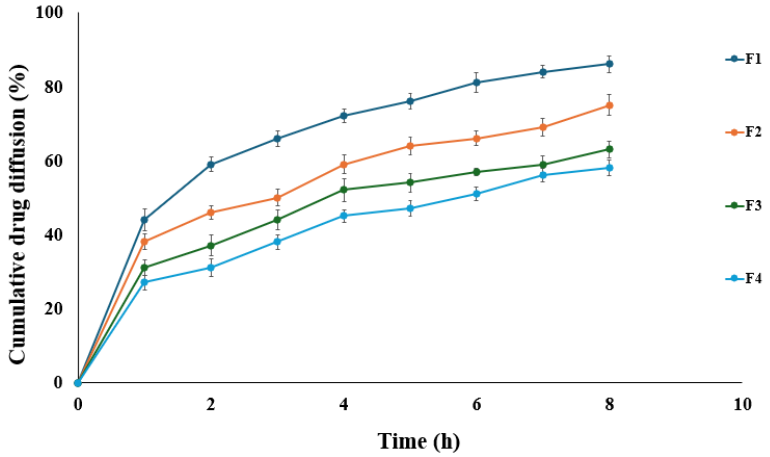

Figure 3. *In vitro* diffusion study of microemulsion, indicating drug diffusion from F1 to F4 formulations, formulation F1 showed higher drug diffusion as compared to F4.

As oil content increased from F1 to F4, a gradual decrease in drug diffusion was observed. Higher oil content leads to greater solubilization of the drug in the oil phase, thereby reducing its thermodynamic activity and its diffusion from the formulation. These results were consistent with those of Alkhaldi *et al*. (2025), who reported enhanced curcumin release with increased water content [31].

3.4.3. Analysis of particle size, PDI, and zeta potential.

These studies were carried out to analyze the colloidal characteristics of luliconazole-loaded microemulsion. Particle size of formulation F1 was 187.9±1.23nm, which was closer to the standard microemulsion particle size (10-200 nm) [32]. PDI serves as an indicator of globule size uniformity in formulation, with values between 0.0 and 1.0. Lower PDI values, approaching 0.0, signify a narrower size distribution and greater homogeneity of the microemulsion system. The polydispersity index of the optimized formulation was 0.2493 in Figure (A), which indicates that the prepared microemulsion showed a narrow size distribution. The zeta potential value of the F1 formulation was -34mV in Figure 4(B). Negative zeta potential is primarily attributed to the non-ionic nature of Labrasol and Labrafil M 2125 CS, which allows adsorption of hydroxyl ions (OH^-) from the aqueous phase onto the surface of oil droplets. Additionally, components of lemongrass oil, such as citral and geraniol, carry partial negative charges or undergo ionization in aqueous environments, further contributing to the negative surface charge. Typically, stable microemulsion systems showed zeta potential values more than±30Mv. These results were found to be approximately similar to the results reported by Laxmi *et al*. (2015) for nanoemulsion of artemether [33]. On this basis, the F1 formulation indicated a stable microemulsion.

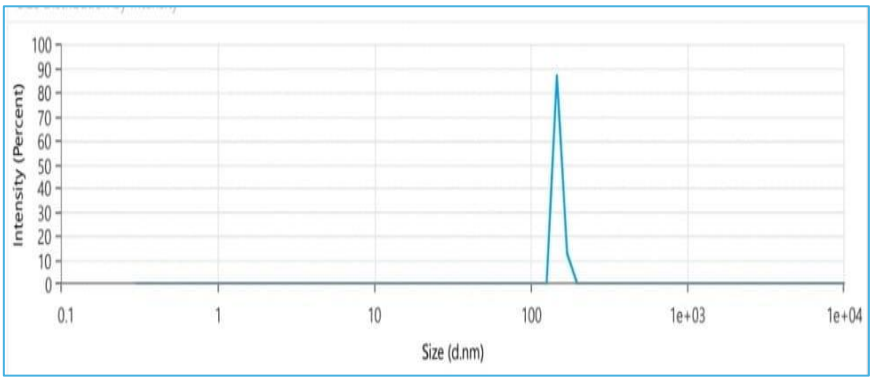

(A)

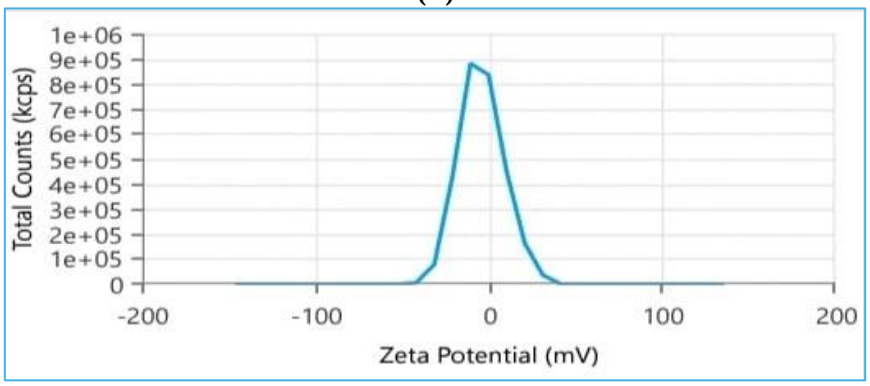

(B)

Figure 4. (A) particle size; **(B)** zeta potential of optimized F1 formulation, indicating the particle size of 187.9 nm and zeta potential of -34mV.

3.4.4. Differential scanning calorimetry (DSC).

The melting point and physical state of luliconazole were assessed by DSC in a microemulsion formulation. Figure 5(A) presents a thermogram of pure luliconazole, which shows a distinct endothermic peak near 153°C. This peak corresponds to the drug's melting point as reported by Chatur *et al*. (2025) [34], confirming its crystalline nature. In contrast, the thermogram of microemulsion in Figure 4(B) did not show the characteristic endothermic peak of luliconazole. This shift indicates successful solubilization of the drug in the microemulsion formulation.

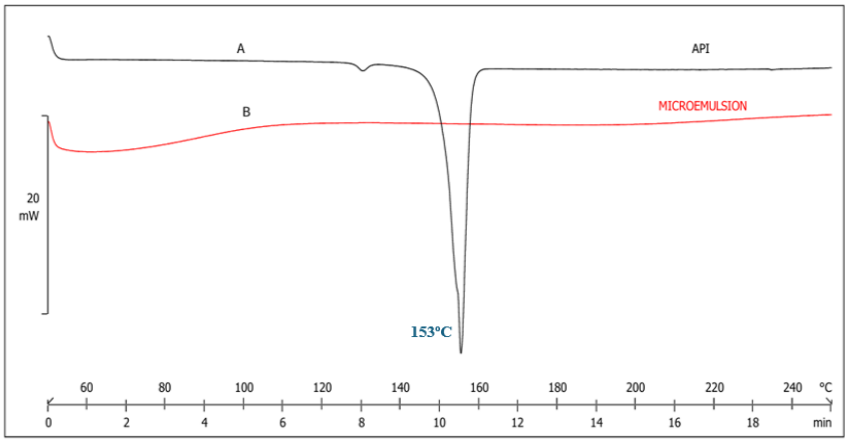

Figure 5. DSC study of **(A)** luliconazole; **(B)** microemulsion formulation, revealing complete solubilization of the drug in the microemulsion as evidenced by the disappearance of the peak of luliconazole.

3.4.5. Scanning electron microscopy (SEM).

SEM image of the microemulsion exhibited a clearly defined spherical morphology with sharp boundaries, suggesting a nearly perfect particle structure, as shown in Figure 6. This characteristic can be attributed to the formation of oil globules that were dispersed in an aqueous environment. Observed morphology resulted from the use of non-ionic surfactants, whose hydrophobic tails turned away from the aqueous phase while hydrophilic heads remained in contact with it. This amphiphilic arrangement promoted the development of distinct, uniformly spherical oil globules in the microemulsion system.

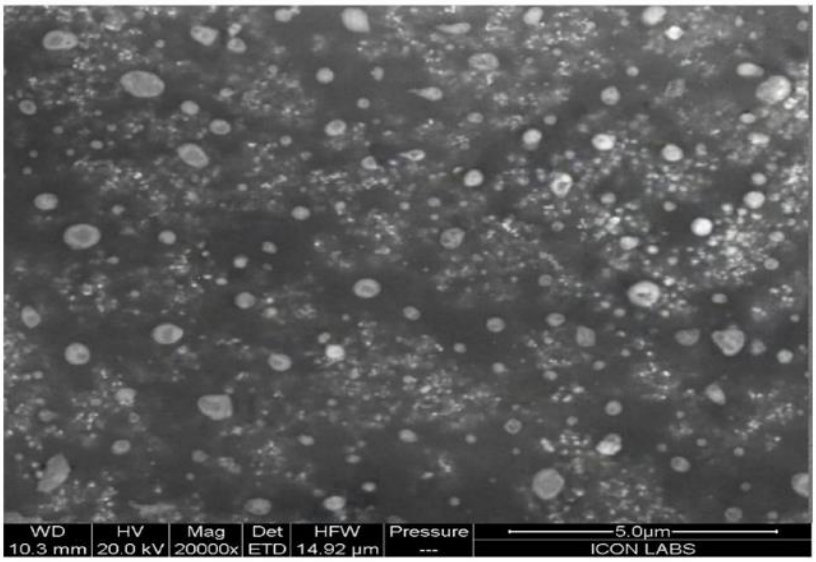

Figure 6. SEM image of microemulsion showing spherical, discrete microemulsion globules.

3.5. Characterization of microemulgel.

3.5.1. pH, viscosity, and drug content.

The microemulgel formulation exhibited a pH of 6.0±0.11, aligning closely with the physiological pH of skin. Maintaining a pH value close to that of normal human skin (around pH 5.5) is particularly important in antifungal gel formulation. A slightly acidic environment not only helps maintain skin health but also inhibits the growth of common fungal pathogens. Viscosity of formulation was 10032±1.5cP. High values of microemulgel confirmed prolonged adhesion of the formulation to skin. Drug content of microemulgel was 98±0.44%, which indicates maximum drug solubility. The high drug content of the microemulgel formulation might contribute to its enhanced therapeutic efficacy.

3.5.2. Texture analysis of microemulgel.

The technique of texture analysis quantifies and evaluates how a material reacts to applied external force. Viscosity, spreadability, ease of removal from containers, and residence time on the skin are important characteristics of topical gels that can be assessed using texture analysis. The force-time plot obtained during texture analysis was used to determine mechanical properties, including firmness, stickiness, and the work done. Firmness of the sample was reflected by the maximum force recorded during the probe's insertion. It measures the sample's deformation under shear. A higher firmness value indicates improved formulation density and uniformity. The maximum negative force measured during probe retraction during the withdrawal phase was used to assess the gel's stickiness or cohesiveness. The hardness of the work done was calculated as the ratio of the area under the firmness curve to the area under the stickiness curve. Figure 7 and Table 4 showed that the marketed gel demonstrated marginally higher firmness, enhanced stickiness, and greater work compared to microemulgel. These observations suggest that the marketed gel is more viscous and less spreadable, whereas the microemulgel enhances user comfort by enabling effortless application and even distribution across the skin.

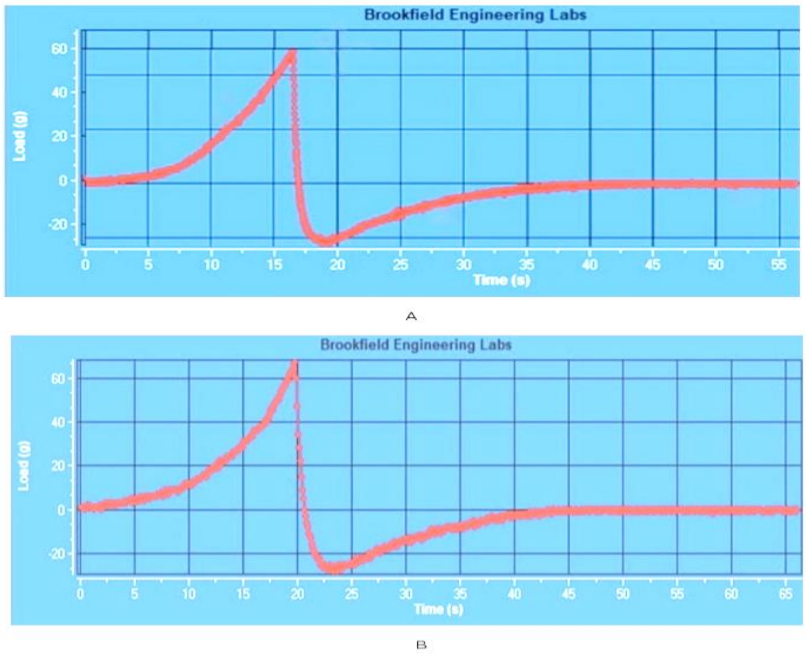

Figure 7. Texture profile analysis of **(A)** microemulgel; **(B)** marketed gel.

Table 4. Spreadability of microemulgel and marketed gel.

Sample	Firmness(g)	Hardness of work done(mJ)	Stickiness(g)
Microemulgel	60±2.14	300±1.43	23±1.24
Marketed gel	64±1.83	320±2.11	24±1.36

The firmness and stickiness of microemulgel and marketed gel were analyzed by an unpaired t-test to determine the significant difference between microemulgel and marketed gel. The result of the firmness demonstrated pooled variance, a t-stat, and p-value of 1, -4.90, and 0.008, respectively. Since the p-value of 0.00805 < 0.05, it signifies a significant difference between microemulgel and the marketed gel. This conclusion is valid with 99% confidence. A t-test was also applied to check the significant difference between these formulations to evaluate stickiness. Results indicated pooled variance, a t-stat, and p-value of 1, 2.77, and 0.29, respectively. Since the p-value of 0.29 >0.05, it signifies no statistical difference between microemulgel and the marketed gel stickiness. The small difference observed (1 unit) could be due to random variation rather than a true effect.

3.5.3. *In-vitro* drug diffusion study.

The Franz diffusion cell apparatus was used to carry out an *in vitro* diffusion study. Drug diffusion from luliconazole-loaded microemulsion, luliconazole-loaded microemulgel, and luliconazole was 86±0.81, 71±0.95, 29±0.69%, respectively, within 8h, as shown in Figure 8. Drug release kinetics from luliconazole-loaded microemulsion, luliconazole-loaded microemulgel, and luliconazole followed Higuchi diffusion kinetics; R^2 values were 0.9664, 0.9969, and 0.9964. Microemulsion showed the highest percent drug diffusion compared to microemulgel and luliconazole, due to the oil phase (lemongrass oil) and surfactants (Labrasol and Labrafil M 2125 CS), which help improve drug solubilization and maintain luliconazole in solubilized form. Luliconazole-loaded microemulgel showed sustained release of the drug over time. This was due to the incorporation of a microemulsion into the gel, which acted as a barrier, slowing the diffusion of the molecule from the formulation and increasing the time of contact between the formulation and the site of application. Limited drug diffusion of luliconazole was observed, attributed to its low aqueous solubility.

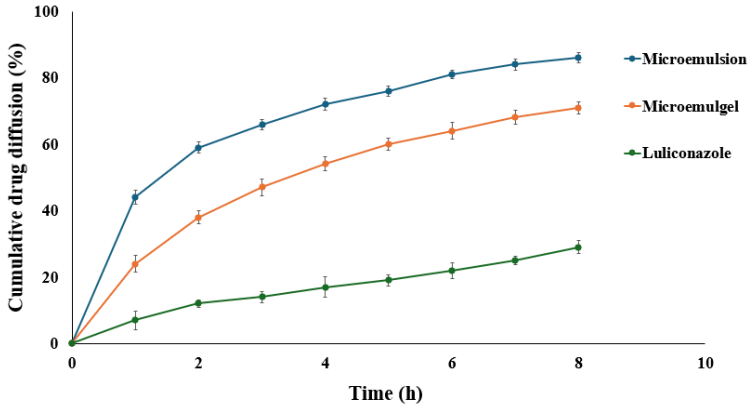

Figure 8. *In-vitro* diffusion study of luliconazole diffusion from microemulsion, microemulgel, and luliconazole, indicating more luliconazole diffusion from microemulgel and restricted drug diffusion from luliconazole-loaded gel.

3.5.4. *Ex vivo* diffusion study.

Goat skin was employed in an *ex vivo* diffusion study to assess drug diffusion. Microemulsion, microemulgel, marketed gel, and luliconazole plain gel showed 79±1.75,

68±2.06, 64±1.97, and 27±1.58% drug diffusion, respectively, in 8 h, as shown in Figure 9. Drug release kinetics from microemulsion, microemulgel, marketed gel, and luliconazole followed Higuchi diffusion kinetics, and R^2 values were 0.9805, 00.9972, 0.9883, and 0.9809, respectively. Microemulsion showed the highest percent drug diffusion compared to microemulgel, marketed gel, and luliconazole-loaded microemulgel. Luliconazole-loaded microemulgel showed sustained drug release over a defined period due to the viscous gel matrix. Luliconazole has low aqueous solubility, and in plain gel, it was present in a partially suspended or crystalline state, limiting diffusion. The absence of solubilizers or penetration enhancers reduces drug diffusion in luliconazole plain gel.

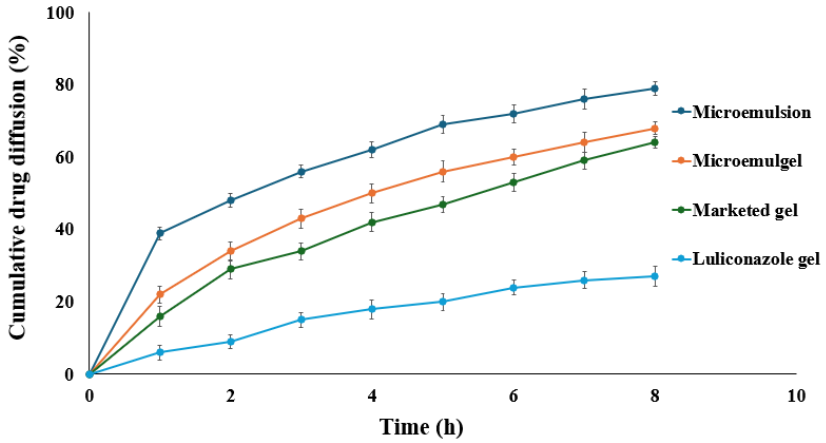

Figure 9. *Ex vivo* diffusion study indicating diffusion of luliconazole from microemulsion, microemulgel, marketed gel, and luliconazole-loaded gel

3.5.5. Antifungal activity.

Antifungal activity of pure luliconazole, lemongrass oil, luliconazole-loaded microemulsion, luliconazole-loaded microemulgel, and marketed gel was performed against *C. albicans* in triplicate (n=3). Figure 10 shows observed inhibition zones.

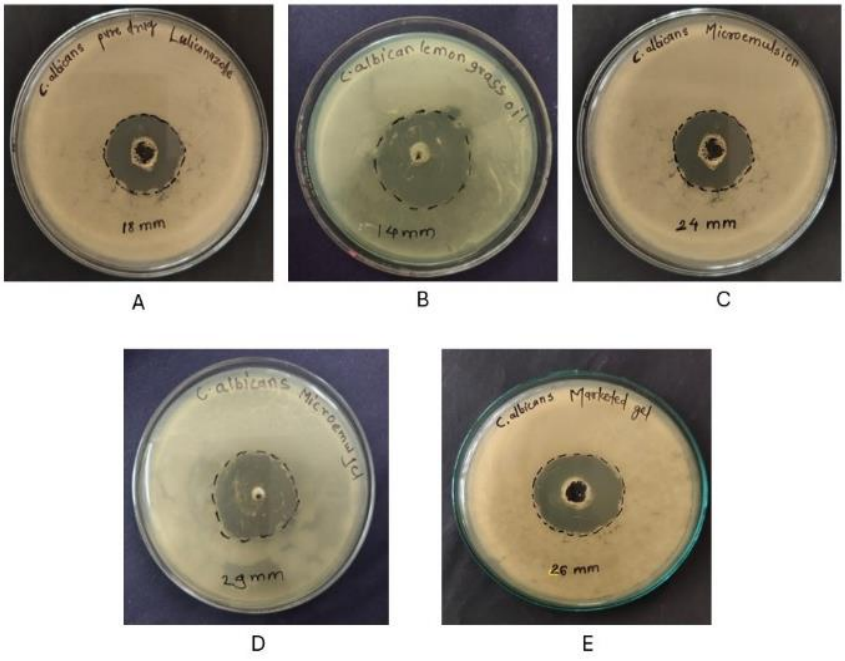

Figure 10. Antifungal activity of **(A)** Luliconazole; **(B)** Lemongrass oil; **(C)** Microemulsion; **(D)** Microemulgel; **(E)** Marketed gel demonstrating antifungal activity of luliconazole and lemon grass oil individually and enhanced activity in the formulation of microemulgel, as well as comparison with the marketed gel against *Candida albicans.*

Diameter of zone of inhibition of pure luliconazole, lemongrass oil, luliconazole-loaded microemulsion, luliconazole-loaded microemulgel, and marketed gel was 18±0.3, 14±0.2, 24±0.6, 29±0.4, and 26±0.4mm, respectively. The zone of inhibition of luliconazole-loaded microemulgel was greater than that of microemulsion and the marketed gel. Microemulgel contains a gel base, which provides sustained drug release. This allows continuous drug availability at the site, maintaining inhibitory concentrations against Candida for longer. Also, the combined effect of luliconazole and lemongrass oil revealed better antifungal activity.

4. Conclusion

Luliconazole-loaded microemulgel was successfully developed using lemongrass oil with a Smix of Labrasol and Labrafil M 2125 CS at a ratio of 7:1. The small globule size of the microemulsion favored availability at the application site, while the microemulgel covered a wider area of the skin for a longer duration, helping prevent fungal infection. A combination of luliconazole with lemongrass oil enhances antifungal activity against *Candida albicans*. Further studies must be conducted for the long-term stability of the formulation and its effectiveness in preclinical and clinical studies.

Author Contributions

Conceptualization, U.K., L.S. and S.M.; methodology, L.S.; software, U.K. and L.S.; validation, U.K., L.S. and S.M.; formal analysis, U.K., L.S. and S.M.; investigation, L.S.; resources, L.S. and U.K.; data curation, L.S. and U.K.; writing—original draft preparation, L.S. and U.K.; writing—review and editing, U.K., L.S. and S.M. All authors have read and agreed to the published version of the manuscript.

Institutional Review Board Statement

Not applicable.

Informed Consent Statement

Not applicable.

Data Availability Statement

No new data were created or analyzed in this study. Data sharing is not applicable.

Funding

This research received no external funding.

Acknowledgement

Authors are grateful to Gattefosse Ltd. for providing a generous gift sample of Labrasol and Labrafil M 2125.

Conflicts of Interest

The authors declare no conflict of interest.

References

1. Hilles, A.; Mahmood, S.; Kaderi, M.; Hashim, R. Review of fungal skin infections and their invasion. *Fungal Territ.* **2019**, *2*, 3-5, https://doi.org/10.36547/ft.2019.2.2.3-5.
2. Bongomin, F.; Gago, S.; Oladele, R. O.; Denning, D.W. Global and Multi-National Prevalence of Fungal Diseases—Estimate Precision. *J. Fungi* **2017**, *3*, 57, https://doi.org/10.3390/jof3040057.
3. Reddy, G K.K.; Padmavathi, A.R.; Nancharaiah, Y.V. Fungal infections: Pathogenesis, antifungals and alternate treatment approaches. *Curr. Res. Microb. Sci.* **2022**, *3*, 100137, https://doi.org/10.1016/j.crmicr.2022.100137.
4. Richardson, J.P.; Ho, J.; Naglik, J.R. Candida-epithelial interactions. *J. Fungi* **2018**, *4*, 22, https://doi.org/10.3390/jof4010022.
5. Metin, A.; Dilek, N.; Demirseven, D.D. Fungal infections of the folds (intertriginous areas). *Am. J. Clin. Dermatol.* **2015**, *33*, 437-347, https://doi.org/10.1016/j.clindermatol.2015.04.005.
6. Ranđelović, M.; Ignjatović, A.; Đorđević, M.; Golubović, M.; Stalević, M.; Rančić, N.; Otašević, S. Superficial candidiasis: cluster analysis of species distribution and their antifungal susceptibility in vitro. *J. Fungi* **2025**, *11*, 338, https://doi.org/10.3390/jof11050338.
7. Doshi, A.; Prabhakar, B.; Wairkar, S. Prolonged retention of luliconazole nanofibers for topical mycotic condition: development, in vitro characterization and antifungal activity against Candida albicans. *J. Mater. Sci. Mater. Med.* **2024**, *35*, 46, https://doi.org/10.1007/s10856-024-06815-w.
8. Mukarram, M.; Choudhary, S.; Khan, M.A.; Poltronieri, P.; Khan, M.M.A.; Ali, J.; Kurjak, D.; Shahid, M. Lemongrass essential oil components with antimicrobial and anticancer activities. *J. Antioxid. Act.* **2021**, *11*, 20, https://doi.org/10.3390/antiox11010020.
9. Ashara, K.C.; Paun, J.S.; Soniwala, M.M.; Chavda, J.R.; Mendapara, V.P.; Mori, N.M. Microemulgel: an overwhelming approach to improve therapeutic action of drug moiety. *Saudi. Pharm. J.* **2016**, *24*, 452-457, https://doi.org/10.1016/j.jsps.2014.08.002.
10. Patel, M.R.; Patel, R.B.; Parikh, J.R.; Patel, B.G. Novel isotretinoin microemulsion-based gel for targeted topical therapy of acne: formulation consideration, skin retention and skin irritation studies. *Appl. Nanosci.* **2016**, *6*, 539-553, https://doi.org/10.1007/s13204-015-0457-z.
11. Firdaus, S.; Hassan, N.; Mirza, M.A.; Ara, T.; El-Serehy, H.A.; Al-Misned, F.A.; Iqbal, Z. FbD directed fabrication and investigation of luliconazole based SLN gel for the amelioration of candidal vulvovaginitis: a 2T (thermosensitive & transvaginal) approach. *Saudi. J. Biol. Sci.* **2021**, *28*, 317-326, https://doi.org/10.1016/j.sjbs.2020.10.005.
12. Alghananim, A.; Özalp, Y.; Mesut, B.; Serakinci, N.; Özsoy, Y.; Güngör, S. A solid ultra fine self-nanoemulsifying drug delivery system (S-SNEDDS) of deferasirox for improved solubility: Optimization, characterization, and in vitro cytotoxicity studies. *Pharmaceuticals* **2020**, *13*, 162, https://doi.org/10.3390/ph13080162.
13. Chen, H.; Chang, X.; Du, D.; Li, J.; Xu, H.; Yang, X. Microemulsion-based hydrogel formulation of ibuprofen for topical delivery. *Int. J. Pharma.* **2006**, *315*, 52-58, https://doi.org/10.1016/j.ijpharm.2006.02.015.
14. Nikumbh, K.V.; Sevankar, S.G.; Patil, M.P. Formulation development, in vitro and in vivo evaluation of microemulsion-based gel loaded with ketoprofen. *Drug Deliv.* **2015**, *22*, 509-515, https://doi.org/10.3109/10717544.2013.859186.
15. Jagdale, S.; Brahmane, S.; Chabukswar, A. Optimization of microemulgel for tizanidine hydrochloride. *Antiinflamm. Antiallergy Agents Med. Chem.* **2020**, *19*, 158-179, https://doi.org/10.2174/1871523018666190308123100.
16. Kumari, P.; Kumar, K.; Joshi, A.; Chauhan, V.; Rajput, V. Development and evaluation of microemulsion formualatons of valsartan for solubility enhancement. *J. Drug Deliv. Ther.* **2023**, *13*, 117-120, https://doi.org/10.22270/jddt.v13i10.5990.
17. Pillai, A.B.; Nair, J.V.; Gupta, N.K.; Gupta, S. Microemulsion-loaded hydrogel formulation of butenafine hydrochloride for improved topical delivery. *Arch. Dermatol. Res.* **2015**, *307*, 625-633, https://doi.org/10.1007/s00403-015-1573-z.
18. Kumar, M.; Shanthi, N.; Mahato, A.K.; Soni, S.; Rajnikanth, P.S. Preparation of luliconazole nanocrystals loaded hydrogel for improvement of dissolution and antifungal activity. *Heliyon* **2019**, *5*, e01688, https://doi.org/10.1016/j.heliyon.2019.e01688.

19. Demirci Kayiran, S.; Guven Bolgen, U.M.; Cevikelli, T.; Kızılyıldırım, S.; Yıldır, B.; Ferahoglu, E.; Kırıcı, S.; Ozogul, F. Chemical composition and antibacterial properties of microemulsion and microemulgel formulations containing lavandula angustifolia mill. essential oils. *Ind. Crop. Prod.* **2025**, *226*, 120654, https://doi.org/10.1016/j.indcrop.2025.120654.
20. Kumari, S.; Alsaidan, O.A.; Mohanty, D.; Zafar, A.; Das, S.; Gupta, J.K.; Khalid, M. Development of soft luliconazole invasomes gel for effective transdermal delivery: Optimization to in-vivo antifungal activity. *Gels* **2023**, *9*, 626, https://doi.org/10.3390/gels9080626.
21. Tartaro, G.; Mateos, H.; Schirone, D.; Angelico, R.; Palazzo, G. Microemulsion microstructure(s): A tutorial review. *Nanomaterials* **2020**, *10*, 1657, https://doi.org/10.3390/nano10091657.
22. Rao, S.; Barot, T.; Rajesh, K.S.; Jha, L.L. Formulation, optimization and evaluation of microemulsion based gel of butenafine hydrochloride for topical delivery by using simplex lattice mixture design. *J. Pharm. Investig.* **2016**, *46*, 1-12, https://doi.org/10.1007/s40005-015-0207-y.
23. Nurman, S.; Yulia, R.; Irmayanti; Noor, E.; Candra Sunarti, T. The optimization of gel preparations using the active compounds of arabica coffee ground nanoparticles. *Sci. Pharm.* **2019**, *87*, 32, https://doi.org/10.3390/scipharm87040032.
24. Kandekar, U.; Lotake, S.; Pandit, A.; Sayare, A.; Ghode, P. Optimization of invasomal gel of miconazole nitrate for the treatment of topical fungal infections. *J. Drug Del. Sci. Technol.* **2025**, 106450, https://doi.org/10.1016/j.jddst.2024.106450.
25. Priyadarshini, P.; Karwa, P.; Syed, A.;Asha, A.N. Formulation and evaluation of nanoemulgels for the topical drug delivery of posaconazole. *J. Drug Deliv. Ther.* **2023**, *13*, 33-43, https://doi.org/10.22270/jddt.v13i1.5896.
26. Makwana, H.; Joshi, D.; Kulkarni, M.; Shah, S.; Acharya, S. Comparative evaluation of clove oil and tea tree oil based topical microemulsion gel in modulating delivery of luliconazole through skin: promising approach for antifungal delivery. *J. Dispers. Sci. Technol.* **2025**, 1-17, https://doi.org/10.1080/01932691.2025.2519387.
27. Ahmad, I.; Farheen, M.; Kukreti, A.; Afzal, O.; Akhter, M.H.; Chitme, H.; Visht, S.; Altamimi, A.S. A.; Alossaimi, M.A.; Alsulami, E.R. Natural oils enhance the topical delivery of ketoconazole by nanoemulgel for fungal infections. *ACS omega* **2023**, *8*, 28233-28248, https://doi.org/10.1021/acsomega.3c01571.
28. Nirmala, M.J.; Mukherjee, A.; Chandrasekaran, N. Improved efficacy of fluconazole against candidiasis using bio-based microemulsion technique. *Biotechnol. Appl. Biochem.* **2013**, *60*, 417-429, https://doi.org/10.1002/bab.1116.
29. Asghar, Z.; Jamshaid, T.; Sajid-Ur-Rehman, M.; Jamshaid, U.; Gad, H.A. Novel transethosomal gel containing miconazole nitrate; Development, characterization, and enhanced antifungal activity. *Pharm.* **2023**, *15*, 2537, https://doi.org/10.3390/pharmaceutics15112537.
30. Alwan, O.M.; Jaafar, I.S. Development of synergistic antifungal in situ gel of miconazole nitrate loaded microemulsion as a novel approach to treat vaginal candidiasis. *Sci. Rep.* **2024**, *14*, 23168, https://doi.org/10.1038/s41598-024-74021-3.
31. Alkhaldi, M.; Sengupta, S.; Keck, C.M. Curcumin microemulsions: influence of compositions on the dermal penetration efficacy. *Pharmaceutics* **2025**, *17*, 301, https://doi.org/10.3390/pharmaceutics17030301.
32. Suhail, N.; Alzahrani, A.K.; Basha, W.J.; Kizilbash, N.; Zaidi, A.; Ambreen, J.; Khachfe, H.M. Microemulsions: Unique properties, pharmacological applications, and targeted drug delivery. *Front. Nanotechnol.* **2021**, *3*, 754889, https://doi.org/10.3389/fnano.2021.754889.
33. Laxmi, M.; Bhardwaj, A.; Mehta, S.; Mehta, A. Development and characterization of nanoemulsion as carrier for the enhancement of bioavailability of artemether. *Artif. Cells Nanomed. Biotechnol.* **2015**, *43*, 334-344, https://doi.org/10.3109/21691401.2014.887018.
34. Chatur, V.M.; Dhole, S.N.; Kulkarni, N.S.; Rudrapal, M. Development and characterization of antifungal niosomal gel of luliconazole: In vitro and ex vivo approaches. *Chem. Phys. Impact* **2025**, *10*, 100801, https://doi.org/10.1016/j.chphi.2024.100801.

Publisher's Note & Disclaimer